

Changes in glacier volume on Mt. Gongga, southeastern Tibetan Plateau, based on the analysis of multi-temporal DEMs from 1966 to 2015

BO CAO, BAOTIAN PAN, WEIJIN GUAN, ZHENLING WEN, JIE WANG

Key Laboratory of Western China's Environmental Systems (MOE), College of Earth and Environmental Sciences, Lanzhou University, Lanzhou 730000, China

Correspondence: Baotian Pan <panbt@lzu.edu.cn>

ABSTRACT. The accelerated retreat of glaciers and the reduction of glacier ice reserves caused by climate change can significantly affect regional water resources and hydrological cycles. Changes in glacier thickness are among the key indicators that reflect this process. We analyzed changes observed in the elevation of glacier surfaces in the Gongga Mountains (GGM) using multi-temporal Digital Elevation Models (DEMs) derived from topographic maps, SRTM, ICESat and ZY-3 data. The results showed that the mean rate of change in glacier surface altitude in the GGM was $\sim -26.7 \pm 2.03$ m (0.54 ± 0.04 m a⁻¹) between 1966 and 2015. The mean melt rates differed over different time periods, latterly showing an accelerating trend. As a general rule, glaciers appear to be losing more volume at lower than at higher elevations. Further analysis of these results suggests that supraglacial debris coverage in the GGM promotes higher rates of mass loss.

KEYWORDS: debris-covered glaciers, glacier mass balance, glacier volume

1. INTRODUCTION

Glaciers have been considered one of the most significant indicators of climate change over recent decades (IPCC, 2013). Most glaciers around the world have retreated significantly as a result of recent climate change (Bolch and others, 2012; Guo and others, 2015), leading to rises in modern sea levels (Gregoire and others, 2012; Jacob and others, 2012; Gardner and others, 2013) and influencing regional hydrological processes in glaciated catchments (Radić and Hock, 2014; Zhang and others, 2015b).

Alongside global climate change, different types of glaciers in different regions show different responses to variations within regional and local climatic regimes. In general, monsoonal maritime glaciers on the Tibetan Plateau (TP) are more sensitive to climate change, and in particular to fluctuations in temperature (Shi and Liu, 2000; Yao and others, 2012; Zhang and others, 2012; Yang and others, 2013; Zhu and others, 2017). However, continental glaciers retreat more slowly (Shi and Liu, 2000; Yao and others, 2012), with a few glaciers even bucking the trend and advancing (Gardelle and others, 2012a; Jacob and others, 2012).

The glaciers on the Gongga Mountains (GGM), on the southeastern margins of the TP, are monsoonal temperate glaciers. Pan and others (2012) determined the extent and rapidity of the change in glacier cover in this area using multi-sourced topographic maps and remote-sensing data. Numerous studies have mentioned the potentially important effects on hydrology of changes in glacier coverage in the GGM as a factor in regional climate change (Li and others, 2010; Pan and others, 2012). Compared to changes in glacier coverage and length, which can be derived relatively easily from remote-sensing data (Paul and others, 2004; Bolch and others, 2010), changes in glacier thickness are

more directly related to changes in a region's glacier mass balance and hydrology (Pieczonka and others, 2013).

Debris-covered glaciers are frequently found in high altitude mountain ranges (Juen and others, 2014). Most glaciers in the GGM are covered by layers of debris. Supraglacial debris cover influences glacier terminus dynamics and can thereby modify a glacier's length response to climate change (Scherler and others, 2011). Thin layers of debris or small single grains absorb more heat than ice, due to their lower albedo. The transfer of this energy into the underlying ice increases ablation rates. However, thicker supraglacial debris cover acts as a protective carapace, insulating the underlying ice and significantly reducing ablation rates (Østrem, 1959; Juen and others, 2014).

Despite the apparent importance of direct mass-balance measurements, only a few records exist for the GGM (e.g. Zhang and others, 2011) due to the inaccessibility of the area and the attendant high labor costs (Ye and others, 2015). Fortunately, remote sensing allows the detection of one or several glacier mass changes at a time through multi-temporal surface digital terrain difference analysis ('the geodetic method'), even in remote mountainous or otherwise unreachable terrains (Paul and Haeberli, 2008). For example, this geodetic method can allow DEMs from the 1950s to the 1980s to be digitized from topographic maps (Xu and others, 2013; Wei and others, 2015). Many scholars have also used declassified KH-9 data to derive DEM values for the 1970s (Pieczonka and Bolch, 2015; Shangguan and others, 2015). Compared to the inevitable historical limitations of such data, satellite imaging techniques such as SPOT HRV (Berthier and Toutin, 2008; Pieczonka and others, 2013), ASTER Terra (Willis and others, 2012; Melkonian and others, 2016) and ALOS

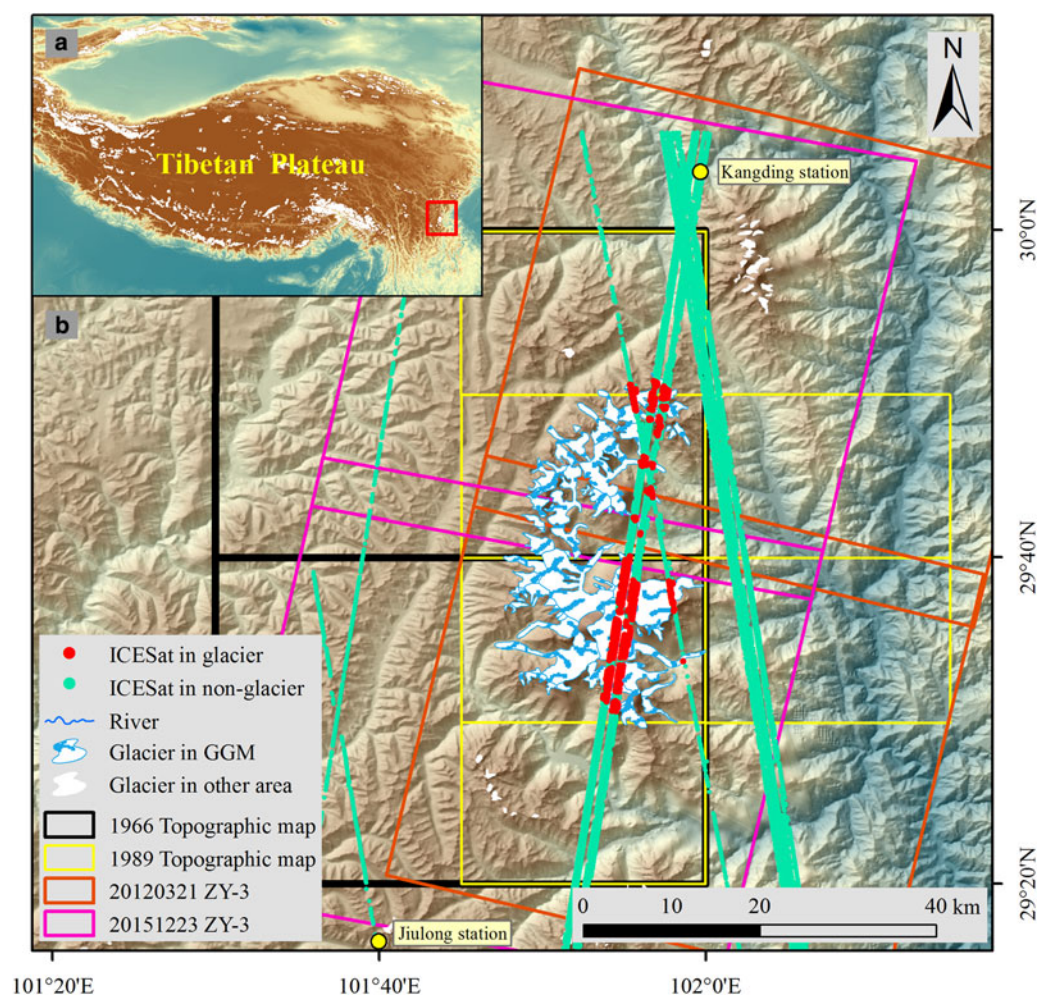


Fig. 1. Location and topography of the Gongga Mountains (GGM). Background: SRTM; glacier outlines based on first CGI. The orange and pink boxes show ZY-3 data coverage from 21 March 2012 and 23 December 2015 respectively.

PRISM (Frey and others, 2012; Ye and others, 2015) can be used for terrain analysis. In 2012, China launched its own ZY-3 earth observation satellite able to provide stereo pairs for DEM generating. In addition, GLAS/ICESat and SRTM data have often been used in glacier coverage reconstructions (Bolch and others, 2013; Neckel and others, 2014). The data from remote sensing is very important for us to understanding the glacier mass-balance change on the TP.

The objectives of this study were to: (1) update decadal-scale changes in glacier coverage using newly-derived boundary data for glaciers from 1966 to 2015; (2) determine any changes in glacier volume and derived mass in the GGM during different time periods using geodetic methods based on a DEM analysis of topographic maps, as well as SRTM, ICESat and ZY-3 data; and (3) investigate the role of debris cover in glaciers mass change in the GGM.

2. STUDY AREA

In 1966, the first Chinese Glacier Inventory (CGI) (Shi, 2008) recorded the GGM region on the southeastern margins of the TP (29–30°N, 101–102°E) (Fig. 1) as having 74 glaciers with a total area of 257.7 km². Most (68%) of the glaciers are covered with debris and the total debris-covered area is ~32 km² (13.5% of the total glacier area of the region (Zhang and others, 2016)). The debris is relatively thin in the upper ablation zones. As the elevation decreases, the

debris thickness increases (Zhang and others, 2011). The glaciers in the GGM are monsoonal temperate glaciers, and are therefore characterized by high flow velocities (~170 m a⁻¹ at 3600 m a.s.l.), high accumulation rates and intense melting (~6000 mm at 3600 m a.s.l.) (Su and others, 1996). Mean annual precipitation (MAP) in this region is ~1930 mm at an altitude of 3000 m a.s.l. on the eastern slopes of the GGM, where the mean annual air temperature (MAT) is ~3.9 °C. According to the record from Gonggasi meteorological station, from May to September, the precipitation accounts for 80% of the whole year (Su and others, 1996). At an elevation of 3700 m a.s.l. on the GGM's western slopes, MAP is ~1150 mm and MAT is ~2.2 °C (Zhang and others, 2015a). The equilibrium-line altitude values are ~4900 and 5100 m a.s.l. for the eastern and western slopes of the GGM, respectively (Shi, 2008). It has been calculated using multi-temporal remote-sensing images (Pan and others, 2012) that the glaciers in the GGM region shrank by ~29.2 km² during the period 1966–2009.

3. DATA SOURCES AND METHODS

3.1. Historical topographic maps

Topographic maps can provide details of glacier surface topography and have been widely used for glaciological purposes (Wei and others, 2015). In this study, two topographic maps

Table 1. Utilized input and reference datasets

Data	Time	Pixel size/scale/footprint	DEM pixel size (m)
Input			
Topographic maps	1966	1: 100 000	30
Topographic maps	1989	1: 50 000	30
ZY3	23 December 2015	2.1 m	10
Reference			
SRTM	February 2000	90 m	30
ICESat	2003–2009	172 m	
ZY3	21 March 2012	2.1 m	10
Landsat OLI	November 2016	30 m	

from 1966 plotted using a scale of 1:100 000, and four topographic maps from 1989 plotted using a scale of 1:50 000, and subsequently acquired by the State Bureau of Surveying and Mapping (Table 1), were used for glacier terrain analysis. We digitized the 20 or 40 m interval contours and spot heights to generate a triangular irregular network map to produce DEM values for the years 1966 and 1989, using the Beijing 1954 datum. Subsequently, the DEMs were re-projected to the UTM coordinate system on the basis of WGS84 datum so as to keep them consistent with other satellite images. During the projection, a seven-parameter datum transformation model with a 30 m resolution was used (Cao and others, 2014). Since the mean slope of the glacierized areas in the GGM is 23°, in accordance with national photogrammetrical mapping standards, the nominal vertical accuracy of these topographic maps with 1:50 000 and 1:100 000 were better than 8 and 16 m, respectively, for the mountain-sides and high mountain areas (with slopes between 6° and 25°) (GB/T12343.1-2008; SAC, 2008).

3.2. SRTM DEM and ICESat GLAS data

The SRTM acquired interferometric synthetic aperture radar (InSAR) data simultaneously in both the C- and X-band frequencies from 11 to 22 February 2000 (Farr and others, 2007). The X-band SAR system was operated with a narrower scan width of only 45 km, leaving large data gaps in the resulting X-band DEM. Such DEM data can be taken as representative of the elevation of glacier surfaces after the 1999 ablation period, with slight seasonal variances (Gardelle and others, 2013; Pieczonka and others, 2013; Shangguan and others, 2015). Fortunately, the entire study region (GGM) was covered by the SRTM X-band. Therefore, in this study, the SRTM X-band was used in order to avoid penetration problems in SRTM C-band by assuming that the penetration depth of the SRTM X-band beam into snow and ice was zero (Gardelle and others, 2012a).

ICESat Global Land Surface Altimetry data products (Zwally and others, 2002; Neckel and others, 2014) provided by the National Snow and Ice Data Center (NSIDC) were also introduced into this study. The height provided in the ICESat GLAS14 was converted to orthometric height using the same reference as the SRTM DEM (referred to WGS84 Ellipsoid and EGM96 Geoid). Bilinear interpolation was used to extract the SRTM surface elevation at the location of each ICESat measurement. The elevation difference (dh) between each ICESat estimate and SRTM DEM represents the thickness change at the sampled footprint. Similar to previous studies, a threshold of 150 m was applied to filter obvious errors of dh due to

cloud cover and atmospheric noise (Kääb and others, 2012; Neckel and others, 2014; Ke and others, 2015).

The accuracy of ICESat elevation footprints has been established as ~10 cm for flat surfaces (Zwally and others, 2008), but is lower for inclined surfaces (Wang and others, 2017). We quantify the combined uncertainty in height change measurements in Section 3.5.

3.3. ZY-3 DEM data

The ZY-3 satellite was launched in 2012 carrying three stereo pair cameras (Forward, Backward, Nadir) with a resolution of 3.5/2.1 m. We collected ZY-3 stereo pair images of two phases (21 March 2012 and 23 December 2015) and then generated the DEM of the study area using the ‘DEM Extraction’ Model provided by the ENVI 5.0 software, using the geographic reference system WGS84 UTM, Zone 47 N. During the DEM generation, at least 20 Ground Control Points (GCPs) for each ZY-3 image were selected. Their coordinates and altitudinal values were derived from Landsat 8 scenes and the DEM data for 1989. Similarly to the SRTM data, the DEM data from the 21 March 2012 ZY-3 images were taken as representative of glacier surface altitudes toward the end of the 2011–2012 accumulation season; the DEM data from the 23 December 2015 ZY-3 images were taken to be indicative of glacier surface altitudes after the 2015 ablation period.

3.4. Glacier boundary inventory and glacier mass change

Pan and others (2012) conducted a systematic study of the glacier coverage in the study area from 1966 to 2009. In this study, we obtained ZY-3 satellite images for 2015 prior to conducting geometric correction and ortho-rectification. Glacier boundaries were digitized using manual methods, and repeatedly verified using imagery in Google Earth.

Changes in glacier surface elevation above sea level were calculated based on area-averaged value *per* 100 m of elevation, using DEM differencing (Xu and others, 2013; Shangguan and others, 2015; Wei and others, 2015).

3.5. DEM co-registration and accuracy

Multi-temporal DEMs require a co-registration to remove the horizontal and vertical offsets before any differential analysis can be performed (Pieczonka and others, 2013). An analytical method proposed by Nuth and Kääb (2011) and later proven as effective by Paul and others (2015) was used in

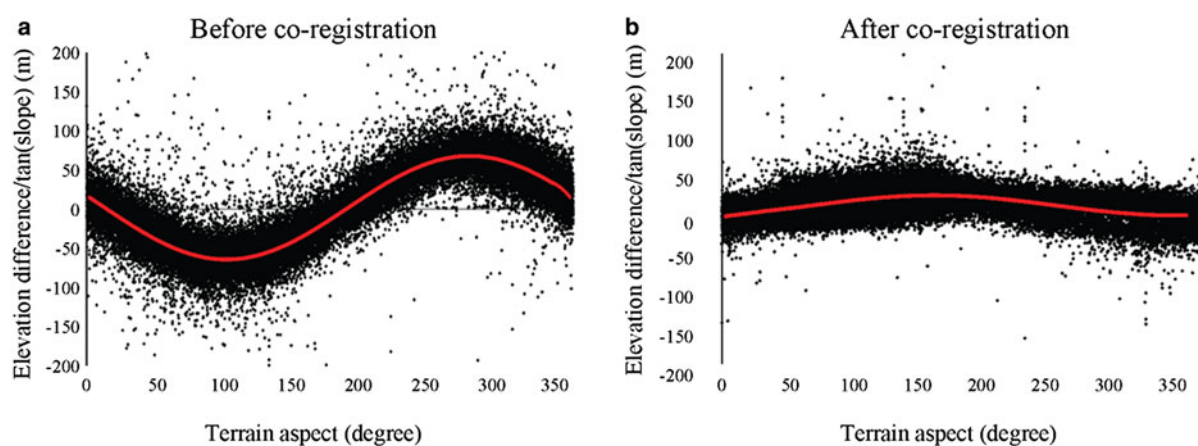


Fig. 2. Scatter plot of slope-standardized altitudinal differences in terrain aspect for off-glacier areas. (a) Before co-registration; and (b) after co-registration (but before optimization using slope aspect).

Table 2. Shift vectors in directions x , y and z (Master DEM > Slave DEM), and uncertainties inherent within non-glaciated areas

Master > Slave	Shift vectors in different directions			Before co-registration		After co-registration and curvature correction	
	X (m)	Y (m)	Z (m)	AD (m)	STD (m)	AD (m)	STD (m)
DEM1989-DEM1966	-54.4	14.8	3.0	6.5	19.4	1.5	15.2
DEM1989-SRTM	36.2	-37.3	-2.4	2.9	29.6	0.2	12.6
SRTM-DEM2015	-41.4	48.2	-35.4	-13.2	21.5	1.9	10.4
SRTM-ICESat	52.8	-23.3	8.5	-7.5	23	0.2	10.8
DEM1989-DEM2015	-5.1	-18.2	-37.2	-18.7	20.8	0.9	11.4
DEM1966-DEM2015	64.8	16.3	16.1	-29.7	32.5	1.2	18.7

AD, mean elevational difference, STD, std dev.

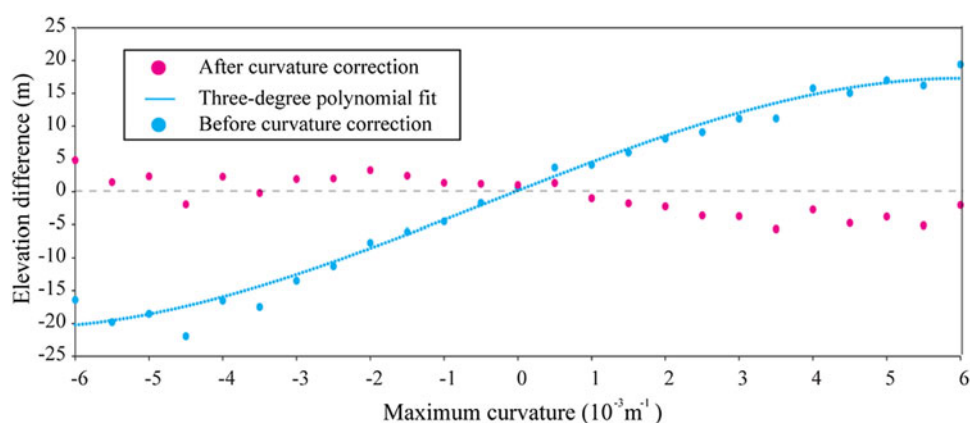


Fig. 3. Relationship between elevation difference and maximum curvature.

this study. All DEMs were bi-linearly resampled to the same cell size of 30 m, and in order to optimize the registration, the observed relationship between DEM altitude differences and aspect in off-glacier areas were used to make further relative adjustments (Fig. 2). Some iterations were built into the registration process where necessary. Extreme outliers were not taken into account and were removed using a threshold method (Berthier and others, 2010; Gardelle and others, 2013). The statistical characteristics evident in these altitudinal differences were used to exclude the pixels that represent altitudinal differences outside the 5–95% range, so as to correct for potential bias (Pieczonka and others, 2013; Wei

and others, 2015). Details of the shifts and errors observed after the abovementioned adjustments were made are listed in Table 2.

We found that even after linear shifting in x , y and z , there is still some obvious elevation difference. As pointed out by previous studies (Berthier and others, 2006; Gardelle and others, 2012b), elevation-dependent vertical bias in mountainous regions is attributable to differences in the original spatial resolution of the two DEMs. The coarse DEM is prone to underestimate the heights of the sharp peaks or ridges with high terrain curvature due to its limited capacity of the representation of high-frequency

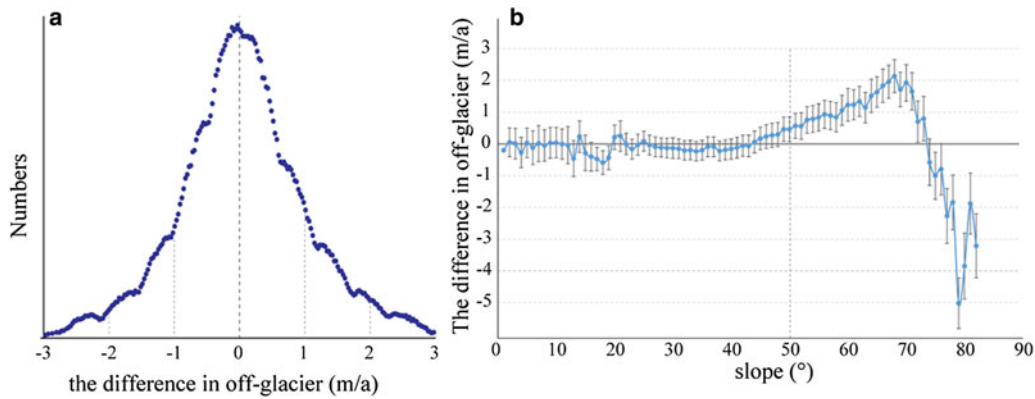


Fig. 4. The final histograms of the difference in off-glacier (a), and the relationship between elevation difference in off-glacier and slope (b).

changes in slopes. This bias can be corrected by the relationship between elevation difference and maximum curvature over the stable terrain off glaciers (Gardelle and others, 2012b, 2013). A clear polynomial relationship is found between the two variables, and thus in this study, a three-degree polynomial fitting is utilized to make the correction (Fig. 3).

After the adjustments, the off-glacier errors are mostly distributed between -1 and 1 m/a (Fig. 4a) and that the large errors are found on steep slopes $>50^\circ$ (Fig. 4b) and therefore do not affect the glacier height change measurements. Then, we estimated the uncertainty in the differences between each pair of DEMs

by using the normalized median absolute deviation (expressed by $1.4826 \times \text{MED}(|\bar{x} - x_i|)$; x_i : elevation difference; \bar{x} : median) (Höhle and Höhle, 2009; Shanguan and others, 2015; Zhang and others, 2018) for the non-glaciated areas (Table 2).

To convert elevation change to mass change, an assumption is required about ice density. A density of $850 \pm 60 \text{ kg m}^{-3}$ was used (cf. Huss, 2013). The final mass-balance uncertainty (E) was calculated as (Zhang and others, 2018):

$$E = \sqrt{\left(\frac{\text{NMAD}}{t} \times \frac{\Delta\rho}{\rho_W}\right)^2 + \left(\frac{\text{NMAD}}{t} \times \frac{\rho_I}{\rho_W}\right)^2} \quad (1)$$

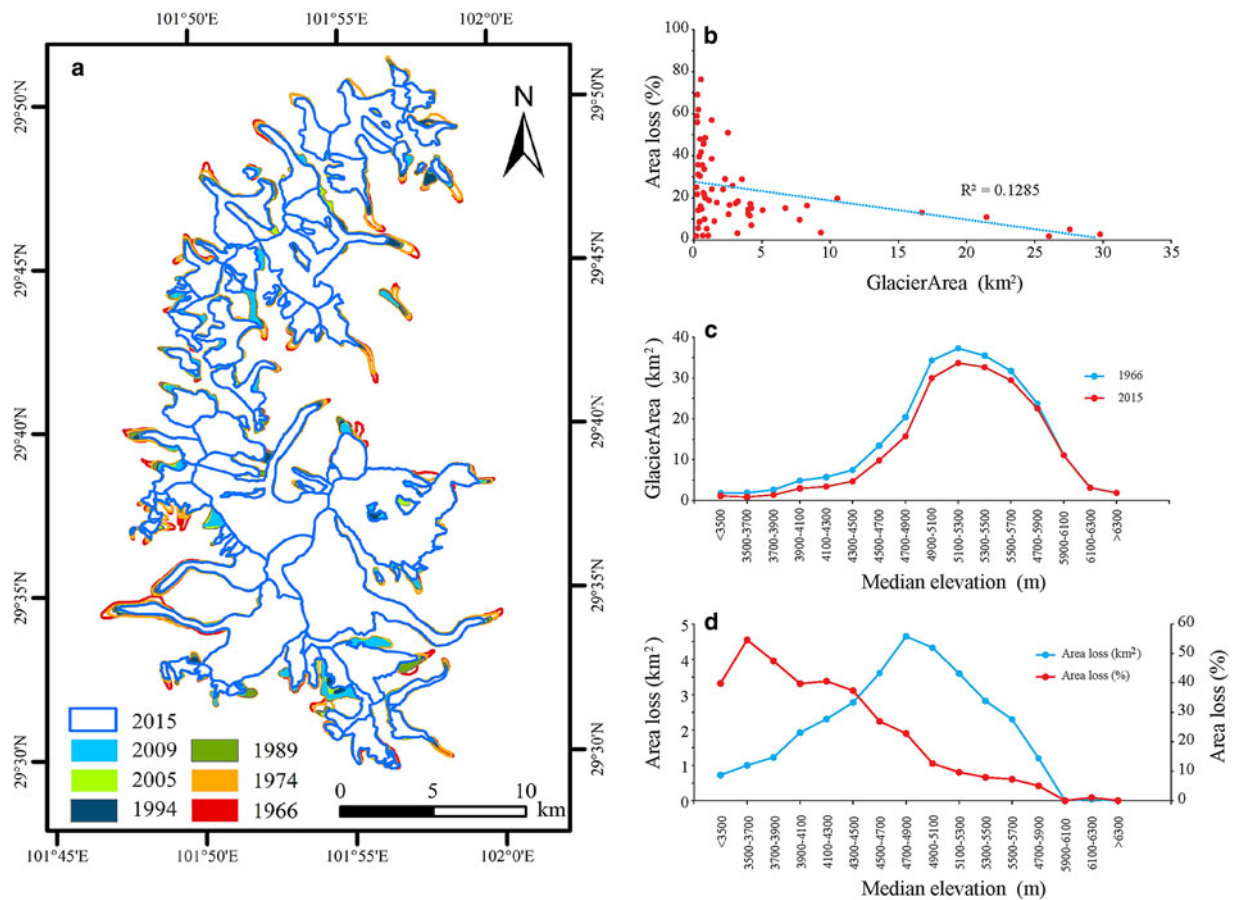


Fig. 5. (a) Glacier boundaries in the GGM for 1966, 1974, 1989, 1994, 2005, 2009 and 2015. (b) Scatter plot of initial glacier area in 1966 versus area loss as a percentage of this initial glacier area between 1966 and 2015. (c) Glacier area at different median altitudes for 1966 and 2015. (d) Area loss in different median altitudes.

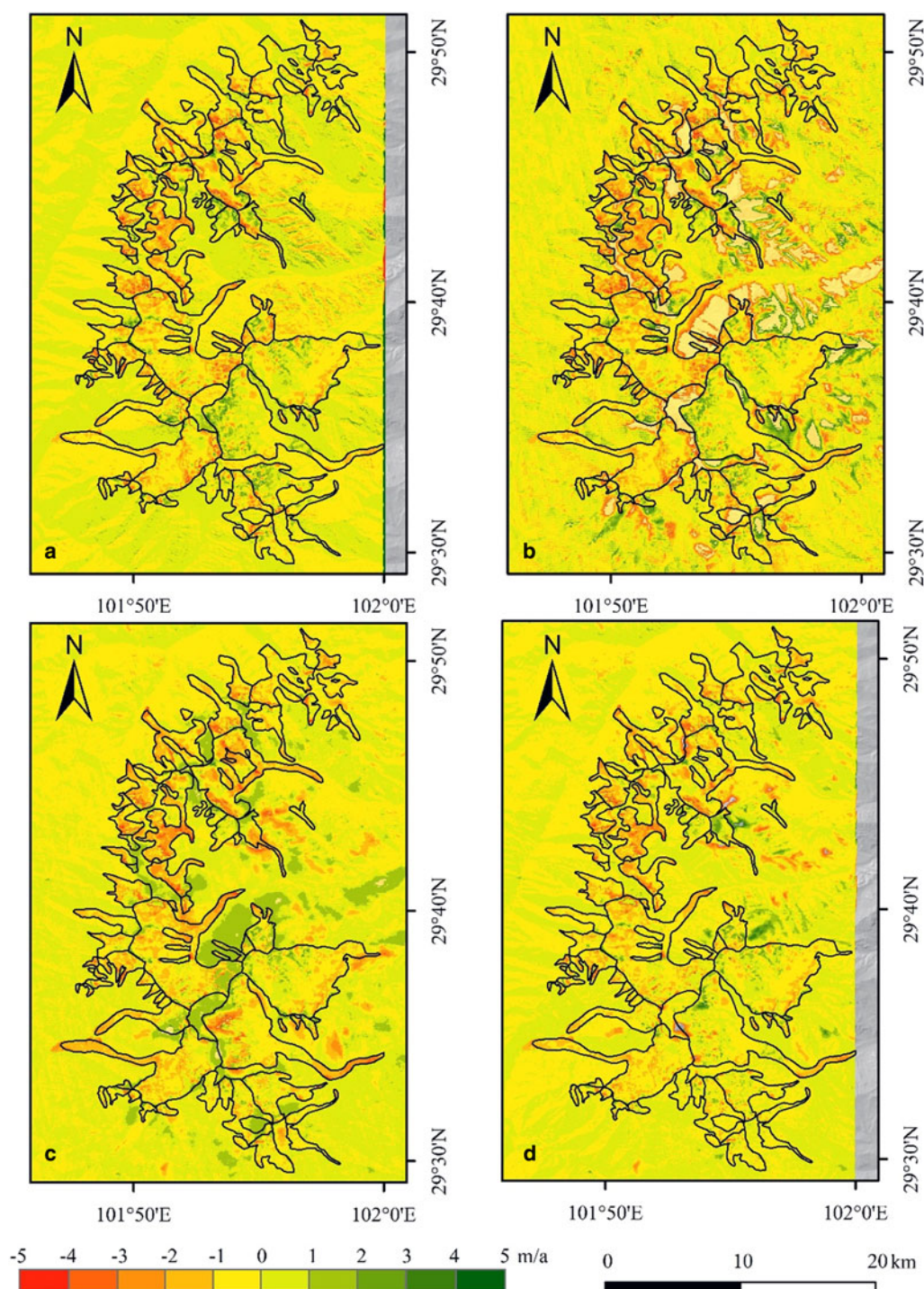


Fig. 6. Differences in glacier surface elevation above sea level over time periods of different lengths, after relative adjustments: (a) 1966–1989; (b) 1989–1999; (c) 1999–2015; and (d) 1966–2015. The large errors visible in the DEM difference figures are found on steep slopes (see Fig. 4).

where t is the observation period, ρ_i the ice density (850 kg m^{-3}), $\Delta\rho$ the ice density uncertainty (60 kg m^{-3}), ρ_w the water density (999.92 kg m^{-3}) (Pieczonka and Bolch, 2015; Zhang and others, 2018).

4. RESULT

4.1. Changes in glacier coverage in the GGM

Pan and others (2012) found that glacier coverage in the GGM had shrunk from 257.7 km^2 in 1966 to 228.5 km^2 in 2009. Our study confirms that the glaciers in this region continued to retreat to a total coverage of $\sim 224.7 \text{ km}^2$ in 2015.

From 1966 to 2015, glacier coverage decreased by 33.0 km^2 (Fig. 5a). Glacier area on the east and west slopes of the GGM decreased by 11.7 and 13.6% since 1966, respectively.

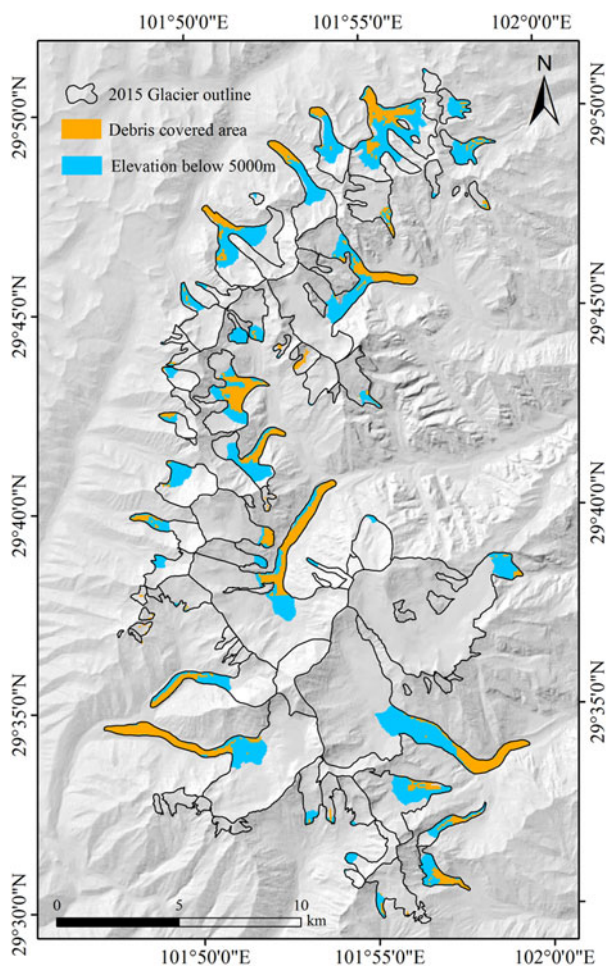
The percentage and rate of area loss were greater for smaller glaciers than for the larger glaciers. A non-linear relation was found between the initial glacier area and glacier area loss as a percentage of this initial glacier area (Fig. 5b). Furthermore, the maximum percentage glacier area loss of $\sim 40\%$ occurred below 4000 m a.s.l. , and as elevation increased, this percentage decreased. Conversely, the actual size of glacier area loss, due to the distribution of glaciers in this region, was found to be greater at higher altitudes,

Table 3. Glacier mass changes in the GGM, 1966–2015

Time period	Changes in mean glacier surface elevation (m)	Rate of change in elevation (m a^{-1})	Glacier mass changes (m w.e. a^{-1})
1966–1989	-8.62 ± 1.68	-0.37 ± 0.07	-0.31 ± 0.06
1989–1999	-6.02 ± 0.49	-0.60 ± 0.05	-0.51 ± 0.04
1999–2015	-12.2 ± 1.88	-0.76 ± 0.12	-0.65 ± 0.10
1989–2015	-17.9 ± 0.87	-0.69 ± 0.03	-0.59 ± 0.03
1966–2015	-26.7 ± 2.03	-0.54 ± 0.04	-0.46 ± 0.04

Table 4. Changes in GGM glacier elevation using ICESat data in comparison with SRTM data

Date	Number of ICESat data	Mean altitude (a.s.l.)	Elevation range	Elevation change	Mass change (m w.e. a^{-1})
15 November 2003	25	5102	3819–6469	-2.40	-0.51 ± 0.27
17 March 2004	25	5136	3834–6526	-2.84	-0.60 ± 0.27
20 November 2005	37	5275	3904–6415	-3.37	-0.48 ± 0.24
23 March 2006	23	5206	3789–6538	-2.56	-0.36 ± 0.24
17 March 2008	27	5181	3788–6537	-4.70	-0.50 ± 0.19
18 March 2009	46	5071	3279–6027	-6.36	-0.60 ± 0.18
Mean		5162			-0.50 ± 0.18

**Fig. 7.** Spatial distributions of debris-covered glaciers in the Gongga Mountains where glacier surface altitudes are <5000 m a.s.l.

with the maximum area loss occurring in the 4900–5100 m band (Figs 5c, d). Above this altitude, the amount of area loss decreased as altitude increased. What is more, when the altitude reached ~ 5900 m a.s.l., the amount of glacier

area loss and the glacier area loss percentage both fell to 0, indicating that the study area's glaciers that are found at altitudes of >5900 m a.s.l. remained relatively stable between 1966 and 2015.

4.2. Changes in glacier surface elevation

Most of the glaciers in the region appear to show a significant surface lowering in ablation region of -26.7 ± 2.03 m ($-0.54 \pm 0.04 \text{ m a}^{-1}$) for the 1966–2015 period (Fig. 6), with an average of -0.51 ± 0.04 and $-0.60 \pm 0.04 \text{ m a}^{-1}$ on the east and west slopes, respectively. Glacier mass decreased by $6.08 \pm 0.53 \text{ km}^3 \text{ w.e.}$ in the study area, although the glacier thickness reduction rate was not consistent over different time periods. Generally speaking, the glacial thinning rate in the GGM is accelerating. During the 1966–1989 period, the glacier mass budget was $-0.31 \pm 0.06 \text{ m w.e. a}^{-1}$; during the 1989–1999 period, it was $-0.51 \pm 0.04 \text{ m w.e. a}^{-1}$; and during the most recent 1999–2015 period, it rose to $-0.65 \pm 0.10 \text{ m w.e. a}^{-1}$ (Table 3).

Determining the factors which control glacier ablation is more difficult, as, along with melt mode, they are highly complex, and produce different levels of melt in different areas. As a general rule, glacial thinning is at its maximum at low elevations, and at its minimum at higher altitudes (Barrand and others, 2010). The lower elevation segments of GGM glaciers have a relatively high melt rate, averaging $-0.81 \pm 0.04 \text{ m a}^{-1}$ below 5000 m a.s.l. for the period 1966–2015. Comparing ICESat and SRTM data, the mean loss of glacier was $0.50 \pm 0.18 \text{ m w.e. a}^{-1}$ for the period 1999–2009 (Table 4).

Supraglacial debris cover may influence loss of glacial mass in glacier ablation region. In the GGM, 68% of the region's glaciers are debris-covered, where the debris-covered proportions of total glacier area vary from 1.74 to 53.0% (Zhang and others, 2016). Using Google Earth imagery, a secondary CGI and the data from Zhang and others (2016), we reconstructed a debris-covered glacier

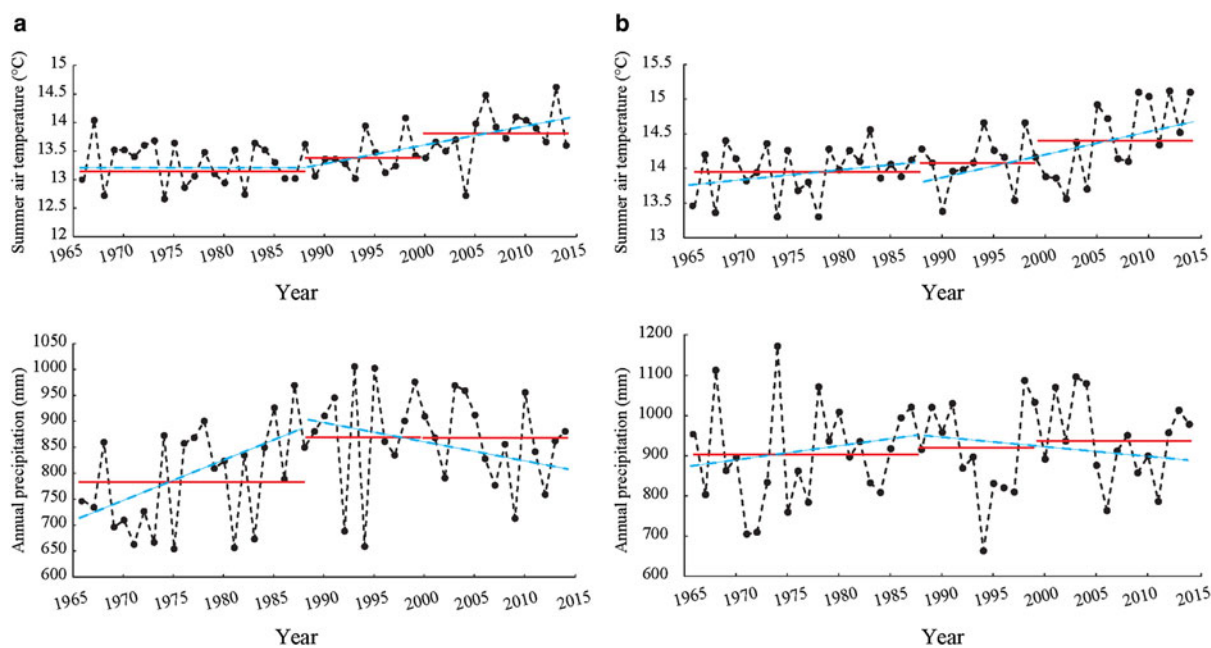


Fig. 8. Changes in annual summer (June to August, inclusive) air temperature and annual precipitation values derived from the (a) Kangding and (b) Jiulong meteorological station datasets. The red line represents the mean value for the different time periods; the blue dashed line is the linear trend line.

map of the GGM (Fig. 7). The rate of change in the mean glacier surface altitude was $-0.54 \pm 0.04 \text{ m a}^{-1}$ over the 1966–2015 period in the study area. The areas where debris-covered glaciers predominate experienced a rate of change of $-0.94 \pm 0.04 \text{ m a}^{-1}$ in 1966–2015. Almost all the debris-covered glaciers in the GGM are distributed at $<5000 \text{ m a.s.l.}$ However, the rate of change in the mean surface elevation for debris-free glaciers found at similar elevations was $\sim -0.78 \pm 0.04 \text{ m a}^{-1}$. It is therefore reasonable to assume that glacial debris cover in the GGM may exert an accelerated effect on glacier melt similar to that found by Zhang and others (2016).

5. DISCUSSION

From 1966 to 2015, glacier mass loss in the GGM was $-0.46 \pm 0.04 \text{ m w.e. a}^{-1}$. This result represents a similar result to that found by Zhang and others (2012), who recorded a mean loss in glacier thickness of $-0.42 \text{ m w.e. a}^{-1}$ in the Hailuoguo catchment using an energy mass-balance modeling method for the period 1952–2009. Our result shows that glacier thickness at low elevations changes at a rate of $0.81 \pm 0.04 \text{ m a}^{-1}$, which was similar to the GPS observation results recorded by Zhang and others (2010) and Zhang and others (2015a).

We compared ICESat and SRTM data to obtain a mean glacier elevation change rate of $-0.50 \pm 0.18 \text{ m w.e. a}^{-1}$ for the period from 1999 to 2009. According to analyses of ICESat data employed in this study, the glacier elevation change rate observed is larger than that seen in the Hengduan Mountains (i.e. $-0.40 \pm 0.41 \text{ m a}^{-1}$, Gardner and others, 2013), and slightly smaller than that of $-0.69 \pm 0.36 \text{ m w.e. a}^{-1}$ than observed in the eastern Nyainqentanglha range (a range of the Hengduan Mountains) (Neckel and others, 2014).

Factors that affect glacier change include both external (climatic) and internal (debris cover, glacier size, topography,

etc.) controls. Zhang and others (2015a) pointed out that it is most likely that climate change has led to the retreat of the GGM's glaciers from 1966 until the present day. Though precipitation values increased over the period, it cannot have fully offset the impact on glacier melt caused by rising temperatures (Fig. 8).

During the first period of study (1966–1989), precipitation in the GGM increased, while temperature values remained essentially unchanged. During the next period (1989–2015), precipitation decreased, while the temperature increased at a faster rate than previously (Fig. 8). Therefore, the glacier thinning rate in the period 1989–2015 was larger than over the period 1969–1989. The accelerating glacier thinning rate from 1966–1989 to 1989–1999 and to 1999–2015 may be caused by the mean temperature of these three periods continuing to rise (Fig. 8).

Supraglacial debris may influence any modeling of glacier melt. Zhang and others (2012) proposed that supraglacial debris markedly accelerates any loss in glacier mass, while Juen and others (2014) concluded that melt rates below debris thicker than $\sim 0.1 \text{ m}$ are highly reduced, as the ice is shielded by the debris cover. Zhang and others (2015a) pointed out that the inhomogeneity of debris thickness can lead to a complex pattern of glacier melt, and that there is hence no obvious relation between changes in glacier surface and glacier altitude in debris-covered areas. With reference to our results, however, we would propose that, for the whole of the GGM at least, supraglacial debris appears to play a positive role in promoting glacier melt.

6. CONCLUSION

In this study, we analyzed changes in glacier mass in the GGM region using topographic maps (i.e. for 1966 and 1989), ZY-3 images (i.e. for 2015) and a cross-comparison of ICESat and SRTM datasets. The results showed that glacier coverage in the GGM region has been decreasing

since 1966, and that the total glacier coverage of 224.7 km² observed for 2015 represents a reduction of 33 km², or 12.8%. From 1966 to 2015, the surface altitude of glaciers in the GGM decreased by -26.7 ± 2.03 m (0.54 ± 0.04 m a⁻¹). During the 1969–1989 period, the rate of change in glacier thickness was -0.37 ± 0.07 m a⁻¹; this rate of change was -0.60 ± 0.05 m a⁻¹ for the period 1989–1999; and for the most recent period, i.e. 1999–2015, the rate of change in glacier thickness was -0.76 ± 0.12 m a⁻¹. As a general rule, glacier melt rates were higher at lower elevations than at higher elevations in this region. Additional analysis suggested that the supraglacial debris coverage of glaciers in the GGM region likely promoted glacier melt.

ACKNOWLEDGEMENTS

We thank two anonymous reviewers and scientific editor Hamish Pritchard for valuable insights that greatly strengthened the manuscript. This study was financially supported by the National Natural Science Foundation of China (grant No. 41701057), the Ministry of Science and Technology of the People's Republic of China (grant No. 2013FY111400), and Fundamental Research Funds for the Central Universities (lzujbky-2018-kb33; lzujbky-2017-225).

REFERENCES

- Barrand NE, James TD and Murray T (2010) Spatio-temporal variability in elevation changes of two high-Arctic valley glaciers. *J. Glaciol.*, **56**(199), 771–780 (doi: 10.3189/002214310794457362)
- Berthier E and Toutin T (2008) SPOT5-HRS digital elevation models and the monitoring of glacier elevation changes in North-West Canada and South-East Alaska. *Remote Sens. Environ.*, **112**(5), 2443–2454 (doi: 10.1016/j.rse.2007.11.004)
- Berthier E, Arnaud Y, Vincent C and Rémy F (2006) Biases of SRTM in high-mountain areas: implications for the monitoring of glacier volume changes. *Geophys. Res. Lett.*, **33**(8), 153–172 (doi: 10.1029/2006GL025862)
- Berthier E, Schiefer E, Clarke GKC, Menounos B and Rémy F (2010) Contribution of Alaskan glaciers to sea-level rise derived from satellite imagery. *Nat. Geosci.*, **3**(2), 92–95 (doi: 10.1038/ngeo737)
- Bolch T, Menounos B and Wheate R (2010) Landsat-based inventory of glaciers in western Canada, 1985–2005. *Remote Sens. Environ.*, **114**(1), 127–137 (doi: 10.1016/j.rse.2009.08.015)
- Bolch T and 11 others (2012) The state and fate of Himalayan glaciers. *Science*, **336**(6079), 310–314 (doi: 10.1126/science.1215828)
- Bolch T and 6 others (2013) Mass loss of Greenland's glaciers and ice caps 2003–2008 revealed from ICESat laser altimetry data. *Geophys. Res. Lett.*, **40**(5), 875–881 (doi: 10.1002/grl.50270)
- Cao B and 7 others (2014) Changes in the glacier extent and surface elevation along the Ningchan and Shuiguan river source, eastern Qilian Mountains, China. *Quat. Res.*, **81**(3), 531–537 (doi: 10.1016/j.yqres.2014.01.011)
- Farr TG and 17 others (2007) The shuttle radar topography mission. *Rev. Geophys.*, **45**(2), RG2004 (doi: 10.1029/2005rg000183)
- Frey H, Paul F and Strozzi T (2012) Compilation of a glacier inventory for the western Himalayas from satellite data: methods, challenges, and results. *Remote Sens. Environ.*, **124**(124), 832–843 (doi: 10.1016/j.rse.2012.06.020)
- Gardelle J, Berthier E and Arnaud Y (2012a) Impact of resolution and radar penetration on glacier elevation changes computed from DEM differencing. *J. Glaciol.*, **58**(208), 419–422 (doi: 10.3189/2012JoG11J175)
- Gardelle J, Berthier E and Arnaud Y (2012b) Slight mass gain of Karakoram glaciers in the early twenty-first century. *Nat. Geosci.*, **5**(5), 322–325 (doi: 10.1038/ngeo1450)
- Gardelle J, Berthier E, Arnaud Y and Kääb A (2013) Region-wide glacier mass balances over the Pamir-Karakoram-Himalaya during 1999–2011. *Cryosphere*, **7**(4), 1263–1286 (doi: 10.5194/tc-7-1263-2013)
- Gardner AS and 15 others (2013) A reconciled estimate of glacier contributions to sea level rise: 2003 to 2009. *Science*, **340**(6134), 852–857 (doi: 10.1126/science.1234532)
- Gregoire LJ, Payne AJ and Valdes PJ (2012) Deglacial rapid sea level rises caused by ice-sheet saddle collapses. *Nature*, **487**(7406), 219–222 (doi: 10.1038/nature11257)
- Guo W and 10 others (2015) The second Chinese glacier inventory: data, methods and results. *J. Glaciol.*, **61**(226), 357–372 (doi: 10.3189/2015jog14j209)
- Huss M (2013) Density assumptions for converting geodetic glacier volume change to mass change. *Cryosphere*, **7**(3), 877–887 (doi: 10.5194/tc-7-877-2013)
- Höhle J and Höhle M (2009) Accuracy assessment of digital elevation models by means of robust statistical methods. *ISPRS-J. Photogramm. Remote Sens.*, **64**(4), 398–406 (doi: 10.1016/j.isprsjprs.2009.02.003)
- IPCC (2013) Climate Change 2013, The Physical Science Basis, Working Group I Contribution to the Fifth Assessment Report of the Intergovernmental Panel on Climate Change. WMO / UNEP, Cambridge University Press, Geneva
- Jacob T, Wahr J, Pfeffer WT and Swenson S (2012) Recent contributions of glaciers and ice caps to sea level rise. *Nature*, **482**(7386), 514–518 (doi: 10.1038/nature10847)
- Juen M, Mayer C, Lambrecht A, Han H and Liu S (2014) Impact of varying debris cover thickness on ablation: a case study for Koxkar Glacier in the Tien Shan. *Cryosphere*, **8**(2), 377–386 (doi: 10.5194/tc-8-377-2014)
- Kääb A, Berthier E, Nuth C, Gardelle J and Arnaud Y (2012) Contrasting patterns of early twenty-first-century glacier mass change in the Himalayas. *Nature*, **488**(7412), 495–498 (doi: 10.1038/nature11324)
- Ke L, Ding X and Song C (2015) Heterogeneous changes of glaciers over the western Kunlun Mountains based on ICESat and Landsat-8 derived glacier inventory. *Remote Sens. Environ.*, **168**, 13–23. (doi: 10.1016/j.rse.2015.06.019)
- Li Z and 13 others (2010) Changes of the Hailuoguo glacier, Mt. Gongga, China, against the background of climate change during the Holocene. *Quat. Int.*, **218**(1), 166–175 (doi: 10.1016/j.quaint.2008.09.005)
- Melkonian AK, Willis MJ, Pritchard ME and Stewart AJ (2016) Recent changes in glacier velocities and thinning at Novaya Zemlya. *Remote Sens. Environ.*, **174**, 244–257 (doi: 10.1016/j.rse.2015.11.001)
- Neckel N, Kropáček J, Bolch T and Hochschild V (2014) Glacier mass changes on the Tibetan plateau 2003–2009 derived from ICESat laser altimetry measurements. *Environ. Res. Lett.*, **9**(1), 1–7 (doi: 10.1088/1748-9326/9/1/014009)
- Nuth C and Kääb A (2011) Co-registration and bias corrections of satellite elevation data sets for quantifying glacier thickness change. *Cryosphere*, **5**(1), 271–290. (doi: 10.5194/tc-5-271-2011)
- Østrem G (1959) Ice melting under a thin layer of moraine and the existence of ice cores in moraine ridges. *Geografiska Annaler*, **41**(4), 228–230
- Pan B and 7 others (2012) Glacier changes from 1966–2009 in the Gongga Mountains, on the south-eastern margin of the Qinghai-Tibetan Plateau and their climatic forcing. *Cryosphere*, **6**, 1087–1101 (doi: 10.5194/tc-6-1087-2012)
- Paul F and Haeberli W (2008) Spatial variability of glacier elevation changes in the Swiss Alps obtained from two digital elevation models. *Geophys. Res. Lett.*, **35**(21), L21502 (doi: 10.1029/2008GL034718)
- Paul F, Huggel C and Kääb A (2004) Combining satellite multispectral image data and a digital elevation model for mapping debris-

- covered glaciers. *Remote Sens. Environ.*, **89**(4), 510–518 (doi: 10.1016/j.rse.2003.11.007)
- Paul F and 24 others (2015) The glaciers climate change initiative: methods for creating glacier area, elevation change and velocity products. *Remote Sens. Environ.*, **162**, 408–426 (doi: 10.1016/j.rse.2013.07.043)
- Pieczonka T and Bolch T (2015) Region-wide glacier mass budgets and area changes for the Central Tien Shan between ~1975 and 1999 using Hexagon KH-9 imagery. *Glob. Planet. Change*, **128**, 1–13 (doi: 10.1016/j.gloplacha.2014.11.014)
- Pieczonka T, Bolch T, Junfeng W and Liu S (2013) Heterogeneous mass loss of glaciers in the Aksu-Tarim Catchment (Central Tien Shan) revealed by 1976 KH-9 Hexagon and 2009 SPOT-5 stereo imagery. *Remote Sens. Environ.*, **130**, 233–244 (doi: 10.1016/j.rse.2012.11.020)
- Radić V and Hock R (2014) Glaciers in the earth's hydrological cycle: assessments of glacier mass and runoff changes on global and regional scales. *Surv. Geophys.*, **35**(3), 813–837 (doi: 10.1007/s10712-013-9262-y)
- Scherler D, Bookhagen B and Strecker MR (2011) Spatially variable response of Himalayan glaciers to climate change affected by debris cover. *Nat. Geosci.*, **4**(3), 156–159 (doi: 10.1038/ngeo1068)
- Shangguan DH and 6 others (2015) Mass changes of Southern and Northern Inylchek Glacier, Central Tian Shan, Kyrgyzstan, during ~1975 and 2007 derived from remote sensing data. *Cryosphere*, **9**(2), 703–717 (doi: 10.5194/tc-9-703-2015)
- Shi Y (2008) *Concise glacier inventory of China*. Shanghai Popular Science Press, Shanghai, China
- Shi Y and Liu S (2000) Estimation on the response of glaciers in China to the global warming in the 21st century. *Chin. Sci. Bull.*, **45**(7), 668–672 (doi: 10.1007/BF02886048)
- Standardization Administration of People's Republic of China (SAC) (2008) GB/T 12343.1-2008. *Compilation specifications for national fundamental scale maps – Part 1: compilation specifications for 1: 25 000/1: 50 000/1: 100 000 topographic maps*. General Administration of Quality Supervision, Inspection and Quarantine, Beijing [In Chinese]
- Su Z, Song G and Cao Z (1996) Maritime characteristics of Hailuogou Glacier in the Gongga Mountains. *J. Glaciol. Geocryol.*, **18**, 51–59, In Chinese
- Wang Q, Yi S and Sun W (2017) Precipitation-driven glacier changes in the Pamir and Hindu Kush mountains. *Geophys. Res. Lett.*, **44** (doi: 10.1002/2017GL072646)
- Wei J and 5 others (2015) Changes in glacier volume in the north bank of the Bangong Co Basin from 1968 to 2007 based on historical topographic maps, SRTM, and ASTER stereo images. *Arct. Antarct. Alp. Res.*, **47**(2), 301–311 (doi: 10.1657/AAAR00C-13-129)
- Willis MJ, Melkonian AK, Pritchard ME and Rivera A (2012) Ice loss from the Southern Patagonian Ice Field, South America, between 2000 and 2012. *Geophys. Res. Lett.*, **39**(17), 128–136 (doi: 10.1029/2012GL053136)
- Xu J, Liu S, Zhang S, Guo W and Wang J (2013) Recent changes in glacial area and volume on Tuanjiefeng Peak Region of Qilian Mountains, China. *PLoS ONE*, **8**(8), e70574 (doi: 10.1371/journal.pone.0070574)
- Yang W and 5 others (2013) Mass balance of a maritime glacier on the southeast Tibetan plateau and its climatic sensitivity. *J. Geophys. Res.-Atmos.*, **118**(17), 9579–9594 (doi: 10.1002/jgrd.50760)
- Yao T and 14 others (2012) Different glacier status with atmospheric circulations in Tibetan Plateau and surroundings. *Nat. Clim. Change*, **2**(9), 663–667 (doi: 10.1038/nclimate1580)
- Ye Q and 8 others (2015) Glacier mass changes in Rongbuk catchment on Mt. Qomolangma from 1974 to 2006 based on topographic maps and ALOS PRISM data. *J. Hydrol.*, **530**, 273–280 (doi: 10.1016/j.jhydrol.2015.09.014)
- Zhang Y, Fujita K, Liu S, Liu Q and Wang X (2010) Multi-decadal ice-velocity and elevation changes of a monsoonal maritime glacier: Hailuogou glacier, China. *J. Glaciol.*, **56**(195), 65–74 (doi: 10.3189/002214310791190884)
- Zhang Y, Fujita K, Liu S, Liu Q and Nuimura T (2011) Distribution of debris thickness and its effect on ice melt at Hailuogou glacier, southeastern Tibetan Plateau, using in situ surveys and ASTER imagery. *J. Glaciol.*, **57**(206), 1147–1157 (doi: 10.3189/002214311798843331)
- Zhang Y, Hirabayashi Y and Liu S (2012) Catchment-scale reconstruction of glacier mass balance using observations and global climate data: case study of the Hailuogou catchment, southeastern Tibetan Plateau. *J. Hydrol.*, **444–445**, 146–160 (doi: 10.1016/j.jhydrol.2012.04.014)
- Zhang G and 5 others (2015a) Elevation changes measured during 1966–2010 on the monsoonal temperate glaciers' ablation region, Gongga Mountains, China. *Quat. Int.*, **371**, 49–57 (doi: 10.1016/j.quaint.2015.03.055)
- Zhang Y, Hirabayashi Y, Liu Q and Liu S (2015b) Glacier runoff and its impact in a highly glacierized catchment in the southeastern Tibetan Plateau: past and future trends. *J. Glaciol.*, **61**(228), 713–730 (doi: 10.3189/2015JG14J188)
- Zhang Y, Hirabayashi Y, Fujita K, Liu S and Liu Q (2016) Heterogeneity in supraglacial debris thickness and its role in glacier mass changes of the Mount Gongga. *Sci. China-Earth Sci.*, **59**(1), 170–184 (doi: 10.1007/s11430-015-5118-2)
- Zhang Z and 5 others (2018) Glacier variations at Aru Co in western Tibet from 1971 to 2016 derived from remote-sensing data. *J. Glaciol.*, **64**(245), 397–406 (doi: 10.1017/jog.2018.34)
- Zhu M and 5 others (2017) Differences in mass balance behavior for three glaciers from different climatic regions on the Tibetan plateau. *Clim. Dyn.*, **195**, 1–28 (doi: 10.1007/s00382-017-3817-4)
- Zwally HJ and 15 others (2002) ICESat's laser measurements of polar ice, atmosphere, ocean, and land. *J. Geodyn.*, **34**(3–4), 405–445 (doi: 10.1016/S0264-3707(02)00042-X)
- Zwally HJ, Yi D, Kwok R and Zhao Y (2008) ICESat measurements of sea ice freeboard and estimates of sea ice thickness in the Weddell Sea. *J. Geophys. Res.-Oceans*, **113**, C02S15 (doi: 10.1029/2007JC004284)

MS received 12 March 2018 and accepted in revised form 28 February 2019; first published online 28 March 2019